

NMR Studies of Peptide T, an Inhibitor of HIV Infectivity, in an Aqueous Environment

ANGEL C. DE DIOS,^{a*} DEVIN N. SEARS^{a§} and ROBERT TYCKO^b

^a Department of Chemistry, Georgetown University, 37th and O Streets, Washington, DC 20057, USA

^b Laboratory of Chemical Physics, NIDDK, National Institutes of Health, Bethesda, MD 20892, USA

Received 4 September 2003

Revised 23 December 2003

Accepted 15 January 2004

Abstract: The synthetic octapeptide peptide T (ASTTTNYT) has been shown to interfere with binding of the HIV-1 envelope glycoprotein gp120 to the chemokine receptor R5, thus preventing viral infection. This study investigated the degree of conformational order of two analogs of peptide T, one biologically active (D-Ala peptide T amide) and one inactive (D-Ala, D-Tyr peptide T amide) using nuclear magnetic resonance (NMR) spectroscopy in an aqueous environment, both in solution and in the frozen solid state. Standard solution NMR techniques such as DQFCOSY, HMQC, ROESY and inversion recovery measurements have been utilized to characterize these peptides. Solid state NMR experiments were likewise employed to study the peptides in a frozen glycerol:water mixture. The NMR results indicate that the monomeric form of both peptide T analogs have considerable conformational heterogeneity. Solid state NMR studies indicate aggregation of D-Ala peptide T, possibly into a β -sheet structure, at concentrations higher than 10 mM. Copyright © 2004 European Peptide Society and John Wiley & Sons, Ltd.

Keywords: peptide T; DAPTA; gp120; CCR5; NMR; ROESY; chemokine receptor

INTRODUCTION

HIV-1 infects healthy cells via the chemokine receptor CCR5 (R5) [1]. The infection process is mediated by the viral envelope glycoprotein gp120 [2–4]. It was discovered in 1986 that the chemotactic portion of this protein had the sequence ASTTTNYT, which is located in the V2 region of gp120 [5]. A synthetic analog that will exhibit improved pharmacokinetic properties (same sequence, but with the

D-isomer of Ala1) was then developed. This peptide is claimed to block effectively the receptor sites of gp120 via antagonism of the chemokine receptor R5 [6], thus preventing viral infection [5]. The chemotactic activity of the peptide has been attributed to residues 4–8, referred to as the core pentapeptide [7]. Studies have also shown that variants of this core pentapeptide have a wide range of potencies in preventing the binding of gp120 [8]. This present work was mainly interested in the octapeptides dASTTTNYT and dASTTTNdYT. Both these peptides have the same primary sequence as peptide T, yet the single substitution of D-tyrosine at residue 7 in the second isomer renders it inactive [7–9].

A previous study using nuclear magnetic resonance (NMR) spectroscopy, with deuterated dimethyl sulfoxide (DMSO-d₆) as solvent, has indicated that peptide T assumes a β -turn conformation in the last four residues of the peptide [10]. The conclusions drawn from this previous work have been disputed

*Correspondence to: Angel C. De Dios, Department of Chemistry, Georgetown University, 37th and O Streets, Washington, DC 20057, USA; e-mail: dediosa@georgetown.edu

§ Current address: University of Illinois at Chicago, Department of Chemistry (MC/111), Chicago, IL 60607, USA

Contract/grant sponsor: National Science Foundation; Contract/grant number: CHE-9874424; CHE-9979259.

Contract/grant sponsor: National Institutes of Health.

Contract/grant sponsor: American Chemical Society-Petroleum Research Fund; Contract/grant number: 33906-AC4.

by other NMR studies on aqueous and non-aqueous solutions [11–13] and by modeling studies of the peptide using molecular dynamics simulations [14–17]. The modeling studies indicate that there are several available low energy conformers, of which only a small percentage represent a β -turn motif.

This paper presents the results of NMR studies of two forms of peptide T conducted in an aqueous solution, as well as solid state NMR studies conducted in a frozen glycerol:water solution. From the data described below, it is concluded that both the biologically active form and the inactive form of peptide T are substantially conformationally disordered in aqueous solution. The conformational disorder is dynamic in the liquid state NMR measurements and static in the solid state NMR measurements. This conclusion is based on the observations that the NMR chemical shifts and scalar couplings in the liquid state are indicative of a random coil conformation, that spin relaxation properties in the liquid state are consistent with an unstructured peptide, and that ^{13}C NMR linewidths in the solid state are indicative of conformational heterogeneity.

MATERIALS AND METHODS

D-Ala peptide T Amide (DAPTA) and D-Ala, D-Tyr peptide T Amide (DADTPTA) were synthesized on an Applied Biosystems model 433A automated peptide synthesizer, using standard Fmoc synthesis and cleavage protocols, a Rink amide MBHA resin (Peptides International) and HBTU activation. Solution NMR measurements were performed on unlabeled samples. Solid state NMR measurements were performed on DAPTA with U- ^{15}N , ^{13}C -labeled Asn6 and Tyr7, and on DADTPTA with U- ^{15}N , ^{13}C -labeled Asn6. Uniformly labeled, Fmoc protected L-Asn and L-Tyr were obtained from Cambridge Isotope Laboratories. Samples for solution NMR were prepared by dissolving the peptide in a 50:50 $\text{H}_2\text{O}:\text{D}_2\text{O}$ mixture. The concentration of the samples was approximately 5 mM in a total volume of 0.2 ml. A water susceptibility matched Shigemi sample tube was used to accommodate the small sample volume. Solid state NMR samples were prepared in glycerol:water as described below. To reduce ^1H spin-lattice relaxation times in the frozen solutions to approximately 1 s, $\text{Na}_2[\text{Cu}(\text{EDTA})]$ with a final concentration of 20 mM was added to these samples.

Solution NMR experiments were performed on a Varian Unity INOVA 500 MHz NMR spectrometer

interfaced with a Sun Sparc Station running the Varian VNMR v.5.1 software. The ^1H and ^{13}C chemical shifts were externally referenced to TMS, and the ^{15}N chemical shifts were externally referenced to benzamide. All two-dimensional (2D) spectra were collected in the phase-sensitive mode using the Haberkorn-States hypercomplex method. Low-power presaturation of the residual HDO signal during the repetition delay was used in each spectrum for solvent suppression. All NMR experiments were conducted at 298 K. The DQFCOSY [18], TOCSY [19] and ROESY [20] spectra were recorded as $512 (t_1) \times 4096 (t_2)$ data sets. Each FID was averaged over 36 scans. The TOCSY spectra used the MLEV-17 sequence [19] with a mixing time of 75 ms. Mixing times (τ_m) of 100, 150, 200 and 250 ms were used in the acquisition of the ROESY spectra. The ^{13}C HMQC and HMBC and the ^{15}N HMQC experiments were likewise collected as $512 (t_1) \times 4096 (t_2)$ data sets. These FIDs were also averaged over 36 scans.

Due to the low viscosity of water, which leads to unfavorable correlation times for an eight-residue peptide, no cross peaks were observed in 2D NOESY spectra of DAPTA and DADTPTA. ROESY experiments were therefore conducted in lieu of NOESY experiments.

Solid state NMR measurements were carried out on a Varian/Chemagnetics Infinity-400 spectrometer. The NMR samples were prepared in a mixture of glycerol and water (40:60 by volume). Peptide concentrations of 1 and 16 mM were used. Peptide solutions were pipetted into 6 mm (240 μl sample volume) magic angle spinning (MAS) rotors, frozen by immersion in liquid N_2 , and inserted into the precooled MAS NMR probe. Measurements were performed at a sample temperature of 150 K. ^{13}C NMR spectra were recorded with a cross-polarization (CP) contact time of 2 ms and at a magic angle spinning (MAS) rate of 5 KHz. ^1H decoupling levels were approximately 80 kHz. 2D ^{13}C NMR spectra were obtained with a 2D exchange pulse sequence, using active rotor synchronization to suppress cross peaks among MAS sidebands. The exchange period consisted of 10 ms of ^{13}C - ^{13}C spin diffusion, with no ^1H decoupling or ^{13}C pulses during the exchange period.

RESULTS

The one-dimensional (1D) ^1H NMR spectra of DAPTA and DADTPTA are shown in Figure 1. The chemical shift dispersion in these spectra is such that almost all ^1H resonance assignments could be made.

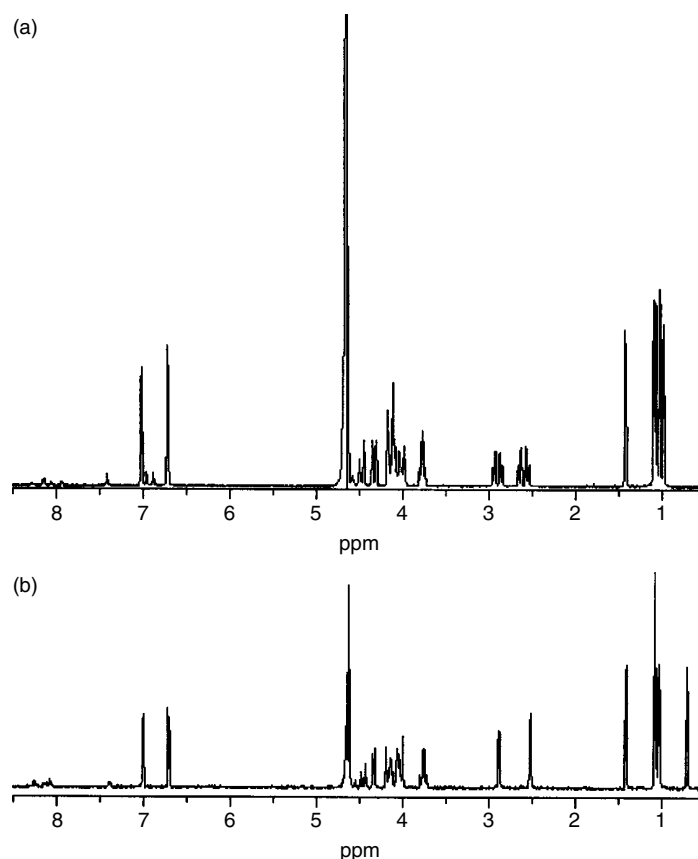


Figure 1 One-dimensional ^1H NMR spectra of (A) D-Ala peptide T and (B) D-Ala, D-Tyr PeptideT in 50% $\text{H}_2\text{O}/50\%$ D_2O at 298 K.

Applying standard methods in assigning spin systems [21], ^1H , ^{13}C and ^{15}N resonance assignments were made using the results from the 2D DQF-COSY, TOCSY, ^{13}C HMQC, ^{13}C HMBC and ^{15}N HMQC experiments. All resonance assignments and J-couplings are listed in Tables 1 and 2 for DAPTA and DADTPTA, respectively. The HN and H^α protons are found to have very similar chemical shifts for the two isomers, indicating very similar conformational distributions. The only substantial difference between the two spectra in Figure 1 is the line for one of the Thr (Thr8) methyl protons. The chemical shift of these protons is around 1.0 ppm in DAPTA, while in DADTPTA a significantly more shielded value is observed, 0.7 ppm. This indicates that the local environment around the γ protons of Thr-8 has changed between the two isomers. The most probable cause of this increase in shielding is the phenyl ring of Tyr7. The side chain of Tyr7 may lie close to the side chain of Thr8 in DADTPTA but significantly further away in DAPTA (because of the different tyrosine enantiomers), suggesting that residues 7 and

8 are assuming an extended conformation in both peptides. Importantly, the backbone chemical shifts ($^{13}\text{C}^\alpha$, $^1\text{H}^\alpha$, $^{13}\text{C}'$, $^{13}\text{C}^\beta$) for both peptides lie very close to those of a random coil [22]. Furthermore, the coupling constants between HN and H^α protons are 6–8 Hz, consistent with a random coil.

Close examination of the ROESY data (Figure 2) suggests that DADTPTA may have a somewhat more rigid structure than DAPTA. More cross peaks are observed in the 2D ROESY spectrum of DADTPTA than in the corresponding DAPTA spectrum. In fact, in Figure 2, before cross peaks can be observed in the DAPTA spectrum, the vertical scale needs to be made so large that the t_1 noise from the water signal is already visible. Interestingly, neither of the two spectra show any $\text{HN}_i \leftrightarrow \text{HN}_{i+1}$ cross peaks, which would be indicative of the type I β -turn [21] reported in the earlier NMR study in DMSO solvent [10]. DADTPTA exhibits the expected sequential cross peaks between HN_i and H_{i-1}^α , as shown in Figure 2. The ROESY spectrum of DADTPTA shows additional cross peaks between Tyr7 HN and Thr4 H^β , and

Table 1 Chemical Shifts (ppm) and Coupling Constants ($^3J_{\text{NH}\alpha}$ Hz) of D-Ala-peptide T in 50% H₂O/50% D₂O

Residue	Position	¹ H chemical shift (ppm)*	¹³ C chemical shift (ppm) ^a	¹⁵ N chemical shift (ppm) ^b	³ J _{NHα} (Hz)
Ala-1	N				
Ala-1	α	4.04	49.30		
Ala-1	β	1.42	16.71		
Ala-1	C		171.38		
Ser-2	N	8.65		117.51	
Ser-2	α	4.45	55.58		6.60
Ser-2	β	3.78	61.21		
Ser-2	C		172.21		
Thr-3	N	8.28		118.46	
Thr-3	α	4.38	59.20		6.43
Thr-3	β	4.19	67.16		
Thr-3	γ 2	1.09	18.98		
Thr-3	C		172.21		
Thr-4	N	8.14		117.89	
Thr-4	α	4.34	59.20		8.35
Thr-4	β	4.15	67.16		
Thr-4	γ 2	1.07	18.92		
Thr-4	C		172.21		
Thr-5	N	8.06		118.55	
Thr-5	α	4.21	59.20		7.48
Thr-5	β	4.02	67.16		
Thr-5	γ 2	0.99	18.87		
Thr-5	C		171.28		
Asn-6	N	8.29		123.26	
Asn-6	α	4.62	50.38		7.72
Asn-6	β	2.61	36.19		
Asn-6	δ 1		172.07		
Asn-6	δ 2	6.76, 7.42			
Asn-6	C		174.45		
Tyr-7	N	8.14		123.49	
Tyr-7	α	4.50	55.43		7.29
Tyr-7	β	2.91	36.17		
Tyr-7	γ		128.17		
Tyr-7	δ	7.01	130.70		
Tyr-7	ϵ	6.71	115.72		
Tyr-7	ζ		154.65		
Tyr-7	C		173.47		
Thr-8	N	7.94		118.38	
Thr-8	α	4.15	58.89		7.97
Thr-8	β	4.14	67.16		
Thr-8	γ 2	1.03	18.87		
Thr-8	C		174.24		
Thr-8	Amide			114.11	

^a Externally referenced to TMS at 0.0 ppm.

^b Externally referenced to benzamide at 105.4 ppm.

between Tyr7 HN and Thr4 H α , suggesting a low population of a turn somewhere between residues 4 and 7. These cross peaks as well as the sequential ones are not observed in DAFTA.

It is important to note that the ROESY cross peaks discussed above for DADTPTA are very weak. The cross peaks in Figure 2B have intensities that are less than 3% of the diagonal peaks.

Table 2 Chemical Shifts (ppm) and Coupling Constants ($^3J_{\text{NH}\alpha}$ Hz) of D-Ala,D-Tyr-peptide T in 50% H₂O/50% D₂O

Residue	Position	¹ H chemical shift (ppm)*	¹³ C chemical shift (ppm) ^a	¹⁵ N chemical shift (ppm) ^b	³ J _{NHα} (Hz)
Ala-1	N				
Ala-1	α	4.04	49.30		
Ala-1	β	1.42	16.72		
Ala-1	C		171.41		
Ser-2	N	8.64		117.57	
Ser-2	α	4.44	55.74		6.48
Ser-2	β	3.77	61.21		
Ser-2	C		172.17		
Thr-3	N	8.26		117.77	
Thr-3	α	4.36	59.25		8.25
Thr-3	β	4.16	67.16		
Thr-3	γ 2	1.08	18.89		
Thr-3	C		172.33		
Thr-4	N	8.19		118.12	
Thr-4	α	4.34	59.25		6.74
Thr-4	β	4.14	67.08		
Thr-4	γ 2	1.07	18.79		
Thr-4	C		172.17		
Thr-5	N	8.08		117.68	
Thr-5	α	4.22	59.25		8.13
Thr-5	β	4.07	67.24		
Thr-5	γ 2	1.04	18.79		
Thr-5	C		171.41		
Asn-6	N	8.28		123.18	
Asn-6	α	4.56	50.74		8.51
Asn-6	β	2.53	36.38		
Asn-6	δ 1		172.34		
Asn-6	δ 2	6.74,7.42			
Asn-6	C		174.28		
Tyr-7	N	8.14		122.90	
Tyr-7	α	4.48	55.91		6.74
Tyr-7	β	2.89	36.22		
Tyr-7	γ		127.91		
Tyr-7	δ	7.01	130.76		
Tyr-7	ϵ	6.71	115.84		
Tyr-7	ζ		154.71		
Tyr-7	C		173.87		
Thr-8	N	8.10		118.45	
Thr-8	α	4.08	58.93		7.27
Thr-8	β	4.01	66.66		
Thr-8	γ 2	0.71	18.47		
Thr-8	C		174.82		

^a Externally referenced to TMS at 0.0 ppm.

^b Externally referenced to benzamide at 105.4 ppm.

Differences between the two spectra in Figure 2 may therefore reflect relatively minor differences in the distributions of conformations adopted by the two peptides in aqueous solution, or differences in the

rates of exchange among populated conformations. Furthermore, the temperature dependence of the amide proton chemical shifts in both peptides is relatively large and negative (about -5 ppb/K).

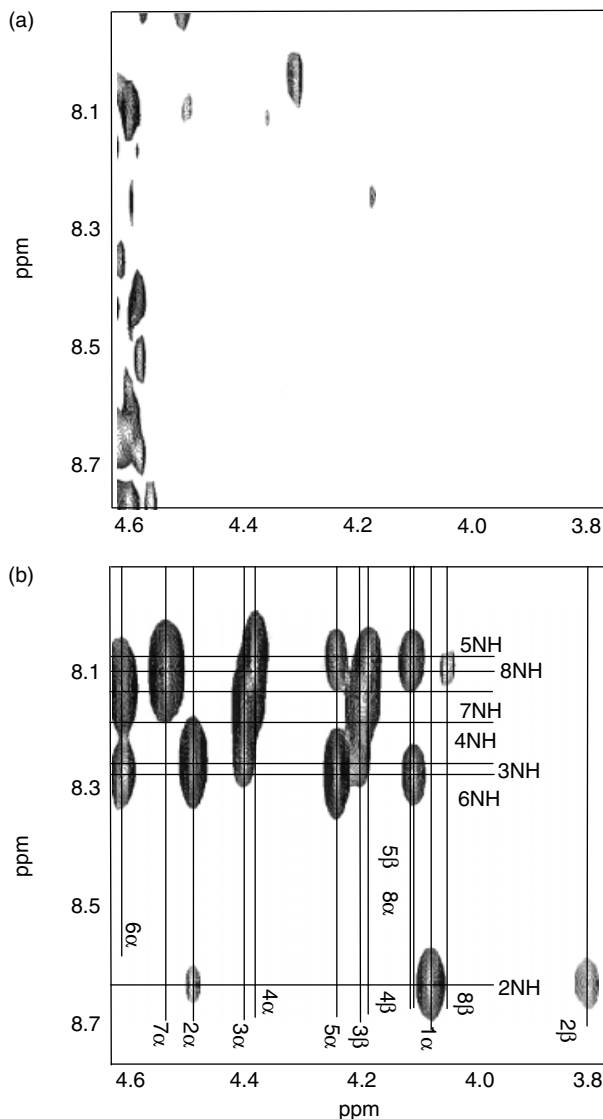


Figure 2 Expansion of the fingerprint region of the ROESY spectra of (A) D-Ala peptide T and (B) D-Ala, D-Tyr peptide T in 50% H₂O/50% D₂O at 298 K. Both spectra are taken under similar conditions but the spectrum in (A) shown here is drawn with a vertical scale 5 times larger than in (B).

This negative temperature dependence coupled with the observed fast exchange of the amide protons with water indicate the absence of intramolecular hydrogen bonding within the peptide [23].

Additional data that support the lack of a rigid structure for DAPTA are provided by ¹³C spin-lattice relaxation time (*T*₁) measurements. A sample with uniformly ¹⁵N, ¹³C-labeled Asn6 and Tyr7 was used in these studies, enabling the direct measurement of *T*₁ via the inversion recovery method for the ¹³C nuclei at these two residues. The results are

Table 3 ¹³C Longitudinal Relaxation Times (*T*₁, s)

	Site	<i>NT</i> ₁ (s) ^a
DAPTA	Asn C'	1.56
	Asn C ^α	0.24
	Asn C ^β	0.23
	Asn C ^γ	2.19
	Tyr C'	1.66
	Tyr C ^α	0.21
	Tyr C ^β	0.31
	Tyr C ^γ	0.67
	Tyr C ^δ	0.26
	Tyr C ^ε	0.26
DADTPTA	Tyr C ^ζ	1.69
	Asn C'	1.53
	Asn C ^α	0.20
	Asn C ^β	0.26
	Asn C ^γ	2.42

^a *N* is the number of hydrogens attached to the C (for unprotonated carbons, *N* = 1).

presented in Table 3. *T*₁ values measured for the protonated backbone ¹³C nuclei do not differ significantly from those of the protonated sidechain sites. Peptides that have a well-defined backbone conformation typically exhibit smaller *T*₁ values for backbone carbon sites than for side chain sites, due to the restricted mobility of the peptide backbone relative to the sidechains. Additionally, the ¹³C *T*₁ values for uniformly labeled Asn6 in DADTPTA are nearly the same as in DAPTA, indicating that the D-Tyr residue in DADTPTA has no significant effect on the dynamics of Asn6. Estimates from the unresolved natural-abundance Thr ¹³C signals for both DAPTA and DADTPTA indicate *NT*₁ (where *N* is the number of hydrogens bonded to the carbon atom, with *N* = 1 for unprotonated carbons) values of 0.26, 0.31 and 1.0 s for the α, β and γ sites, respectively. These values, combined with the observed chemical shifts and coupling constants, strongly suggest the absence of a single molecular conformation that can appropriately describe these peptides and further indicate the absence of major differences in the conformational distributions and dynamics of DAPTA and DADTPTA.

Solid state NMR experiments were performed to further characterize the structural states of the peptides. These experiments were performed at low temperature (150 K) using a glycerol:water mixture to ensure a glassy frozen solution, rather than a polycrystalline state. The addition of glycerol does

not perturb the structure, as 1D and 2D solution NMR spectra of the peptides in glycerol:water were found to be identical to those obtained using water alone as solvent. Two concentrations were used (1 mM and 16 mM) in these solid state NMR studies. Figure 3 compares 1D ^{13}C NMR spectra of 16 mM samples of DAPTA (liquid and frozen glycerol:water solutions) and DADTPTA (frozen solution only). The ^{13}C NMR lines are obviously wider in the frozen solutions (4–5 ppm full width at half maximum) than in liquid state. The sharp lines observed in the liquid state are due to the presence of rapid motional averaging among multiple conformations, which is suppressed in the frozen solutions. ^{13}C linewidths in the frozen solutions are consistent with a significant distribution of conformations for both peptides. Peptides with well-defined conformations in frozen solutions or other noncrystalline environments typically exhibit ^{13}C MAS NMR linewidths in the 1.0–2.5 ppm range [24,25].

The peak at 42 ppm in the solid state NMR spectrum of DAPTA (Figure 3C) is of particular interest, as this peak is anomalously sharp and is not observed in the liquid state (Figure 3A). Additional new peaks are also observed in the C^α and C' regions. These new peaks are also not observed in solid state NMR spectra of the 1 mM sample of DAPTA, indicating that they arise from a DAPTA conformer that corresponds to an aggregated form of the peptide. The resonance near 42 ppm can be assigned to C^β of Asn6 via 2D exchange spectroscopy in the solid state, as shown in Figure 4. The cross peak between the 42 ppm signal and a signal in the C' region establishes this assignment. New cross peaks attributable to the aggregated state of DAPTA are also seen for the $\text{C}'/\text{C}^\alpha$, $\text{C}^\alpha/\text{C}^\beta$ and C^β/C' pairs of Asn6 in Figure 4. This chemical shift for a β -carbon of Asn is highly deshielded, implying backbone dihedral angles characteristic of a β -strand conformation. The chemical shifts for the C' and C^α sites of Asn6 are also consistent with a β -strand conformation. In contrast, neither the 1 mM nor the 16 mM frozen samples of the isomer DADTPTA show additional ^{13}C MAS NMR peaks for Asn6, indicating that DADTPTA does not aggregate at high concentrations in glycerol:water. This observation can be rationalized by the fact that the D -enantiomer of tyrosine disrupts β -sheet formation through unfavorable side chain packing. Thus, although the D -Tyr residue has no major effect on the conformational distribution and dynamics in the monomeric state of peptide T, the D -Tyr residue does affect the propensity to form structurally ordered aggregates.

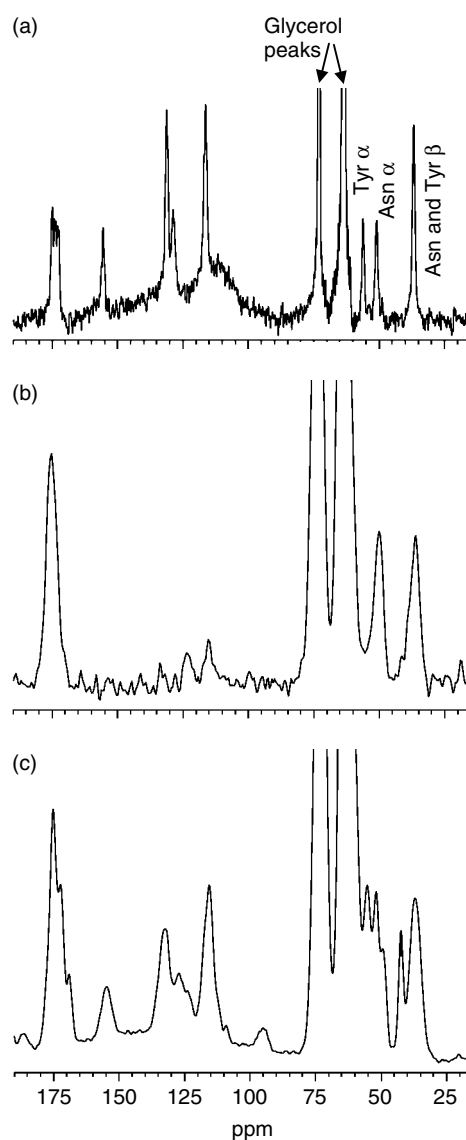


Figure 3 One-dimensional ^{13}C NMR spectra of D -Ala peptide T with uniformly ^{15}N , ^{13}C -labeled Asn6 and Tyr7 (A,C) and D -Ala, D -Tyr peptide T with uniformly ^{15}N , ^{13}C -labeled Asn6 (B). All spectra are from glycerol:water solutions, either in the liquid state at 298 K (A) or in the frozen glassy state at 150 K (B,C).

DISCUSSION AND CONCLUSIONS

1D and 2D NMR experiments were utilized to explore whether peptide T and its D -Tyr analog adopt a preferred structure in solution. The observed chemical shifts and coupling constants, combined with the lack of strong cross peaks in NOESY and ROESY experiments and the measured ^{13}C spin-lattice relaxation times, indicate that both peptides

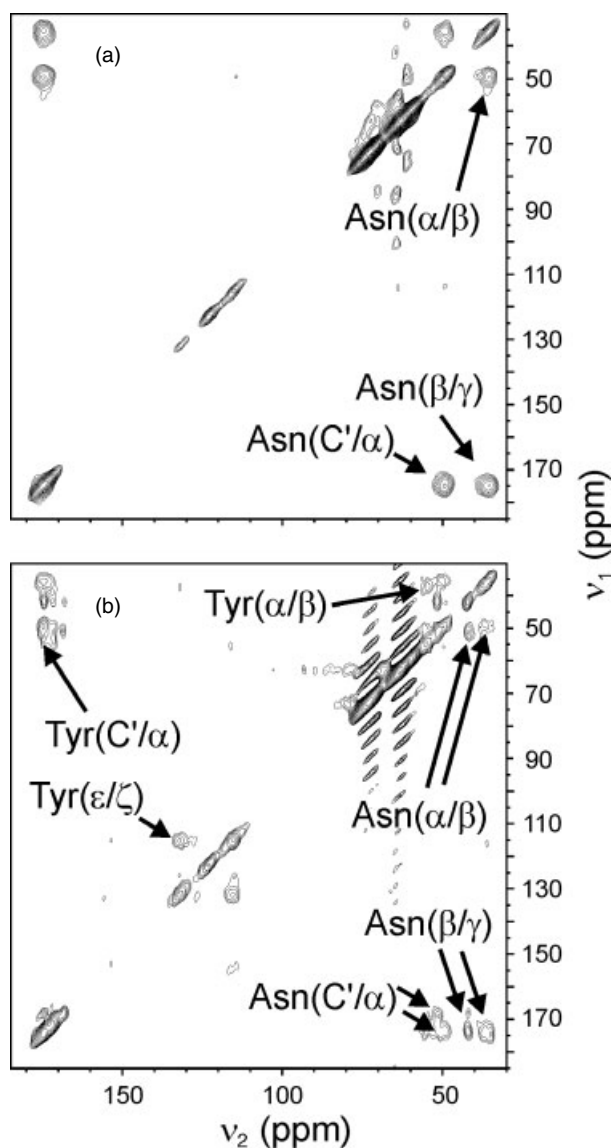


Figure 4 Two-dimensional solid state ^{13}C NMR exchange spectra of peptide T in frozen glycerol:water solution at 150 K. (A) D-Ala, D-Tyr peptide T with uniformly ^{15}N , ^{13}C -labeled Asn6. (B) D-Ala peptide T with uniformly ^{15}N , ^{13}C -labeled Asn6 and Tyr7. Assignments of peptide T crosspeaks are indicated. Spurious crosspeaks between 58 ppm and 75 ppm in v_2 dimension are due to truncation of the intense glycerol signals.

are highly flexible and conformationally disordered in aqueous solution. It is not possible to assign a single structure to these peptides. ^{13}C MAS NMR linewidths observed in 1D and 2D solid state NMR measurements of frozen solutions of these peptides likewise support this conclusion. The decreased potency as an inhibitor of HIV infectivity caused by

the substitution of D-tyrosine in residue 7 of peptide T does not appear to result from a significant change in the conformational state of the free peptide. The decreased potency is probably caused directly by the stereochemistry of the tyrosine side chain. With D-Tyr, it may no longer be possible for the peptide to adopt a conformation in which the Tyr side chain matches the binding site on the chemokine receptor.

The solution NMR results presented above are largely consistent with an earlier study of peptide T by Zangger and Sterk [12], even though the peptide in this earlier study contained no D-amino acids and was not amidated at the C-terminus. ^1H chemical shifts agree to within 0.1 ppm and $^3J_{\text{NH}\alpha}$ coupling constants agree to within 2 Hz. The ^{13}C chemical shift and T_1 data reported above have not been reported in previous studies of peptide T. These data represent significantly new information about the behavior of monomeric peptide T in aqueous solution. In addition, the DAPTA form of peptide T, which has not been previously studied by NMR in aqueous solution, is the form that is currently being considered for clinical applications [26]. Finally, comparisons between the D-Tyr and L-Tyr forms of peptide T, which have dramatically different biological properties [9–11], have not been made in earlier NMR studies.

The solid state NMR evidence given above for β -sheet aggregation of DAPTA at high peptide concentrations is consistent with an earlier report by Millet *et al.* of β -sheet aggregation of peptide T, with no D-amino acids and with acetyl capping of the N-terminus, in DMSO solution [13]. In this earlier report, peptide T was found to be in rapid exchange between random coil and β -sheet forms. In our solid state NMR experiments, the apparent β -sheet form is present as a stable structure and is highly populated (roughly 30%, based on crosspeak volumes in Figure 4.) The effect of D-Tyr on peptide T aggregation has not been observed in earlier NMR studies.

Acknowledgements

DNS was partially supported by NSF grant CHE-9979259. This work was supported in part by a CAREER Award to ACD from the National Science Foundation under Grant No. CHE-9874424 and by a grant to RT from the Intramural AIDS Targeted Antiviral Program of the National Institutes of Health. Acknowledgement is made to the donors of the Petroleum Research Fund, administered by

the American Chemical Society, for partial support of this research. We thank Dr Simon Sharpe for help with solid state NMR spectroscopy and Dr Wa-Ming Yau for help with peptide synthesis. Useful advice and discussions with Dr Michael Ruff and Dr Candace Pert are likewise acknowledged.

REFERENCES

1. Michael NL, Moore JP. HIV-1 entry inhibitors: evading the issue. *Nat. Med.* 1999; **5**: 740–742.
2. Feng Y, Broder CC, Kennedy PE, Berger EA. HIV-1 entry cofactor: functional cDNA cloning of a seven-transmembrane, G protein-coupled receptor. *Science* 1996; **272**: 872–877.
3. Cocchi F, DeVico AL, Grazino-Demo A, Arya SK, Gallo RC, Lusso P. Identification of RANTES, MIP-1 alpha, and MIP-1 beta as the major HIV-suppressive factors produced by CD8+ T cells. *Science* 1995; **270**: 1811–1815.
4. Bleul CC, Farzan M, Choe H, Parolin C, Clark-Lewis I, Sodroski J, Springer TA. The lymphocyte chemoattractant SDF-1 is a ligand for LESTR/fusin and blocks HIV-1 entry. *Nature* 1996; **382**: 829–833.
5. Pert CB, Hill JM, Ruff MR, Berman RM, Robey WG, Arthur LO, Ruscetti FW, Farrar WL. Octapeptides deduced from the neuropeptide receptor-like pattern of antigen T4 in brain potently inhibit human immunodeficiency virus receptor binding and T-cell infectivity. *Proc. Natl Acad. Sci. USA* 1986; **83**: 9245–9258.
6. Redwine LS, Pert CB, Rone JD, Nixon R, Vance M, Sandler B, Lumpkin MD, Dieter DJ, Ruff MR. Peptide T blocks GP120/CCR5 chemokine receptor-mediated chemotaxis. *Clin. Immunol.* 1999; **93**: 124–131.
7. Ruff MR, Martin BM, Girmus EI, Farrar WL, Pert CB. CD4 receptor binding peptides that block HIV infectivity cause human monocyte chemotaxis. Relationship to vasoactive intestinal polypeptide. *FEBS Lett.* 1987; **211**: 17–22.
8. Brenneman DE, Buzy, JM, Ruff MR, Pert CB. Peptide-T sequences prevent neuronal cell-death produced by the envelope protein (gp120) of the human immunodeficiency virus. *Drug Develop. Res.* 1988; **15**: 361–369.
9. Smith CC, Hallberg PL, Sacerdote P, Williams P, Sternberg E, Martin B, Pert C, Ruff MR. Tritiated Dala1-peptide T binding: A pharmacologic basis for the design of drugs which inhibit HIV receptor binding. *Drug Develop. Res.* 1988; **15**: 371–379.
10. Picone D, Temussi PA, Marastoni M, Tomatis R, Motta A. A 500MHz study of peptide T in a DMSO solution. *FEBS. Lett.* 1988; **1**: 159–163.
11. Ojha PR, Saran A, Kamath S, Coutinho E. An investigation of the conformation of peptide-T and its D-Ala analog by NMR and molecular dynamics simulations. *Ind. J. Biochem. Biophys.* 1998; **35**: 133–141.
12. Zangger K, Sterk H. Conformation of peptide T in aqueous solution. Determination of homonuclear coupling constants by selective HOHAHA techniques. *Magn. Reson. Chem.* 1995; **33**: 421–425.
13. Millet O, Pérez JJ, Pons M. An easy NMR method to study the formation of parallel β -sheets in peptide aggregates. *Lett. Pept. Sci.* 1999; **6**: 247–253.
14. Filizola M, Centeno NB, Perez JJ. Computational study of the conformational domains of peptide T. *J. Peptide Sci.* 1997; **3**: 85–92.
15. Andrianov AM, Akhrem AA. Theoretical study of the spatial structure of the Ala-Ser-Thr-Thr-Thr-Asn-Tyr-Thr segment of the HIV gp120 protein, responsible for binding of the virus with the T-cell T4 receptor. *J. Mol. Biol.* 1997; **31**: 180–188.
16. Godjayevev NM, Akyüz S, Akverdieva G. A molecular mechanics conformational study of peptide T. *J. Mol. Struct.* 1996; **403**: 95–110.
17. Centeno NB, Perez JJ. A proposed bioactive conformation of peptide T. *J. Comput.-Aided Mol. Design* 1998; **12**: 7–14.
18. Rance M, Sorensen OW, Bodenhausen G, Wagner G, Ernst RR, Wüthrich K. Improved spectral resolution in COSY 1H NMR spectra of proteins via double quantum filtering. *Biochem. Biophys. Res. Commun.* 1984; **117**: 479–485.
19. Bax A, Davis DG. MLEV-17-based two-dimensional homonuclear magnetization transfer spectroscopy. *J. Magn. Reson.* 1985; **65**: 355–360.
20. Bax A, Davis DG. Practical aspects of two-dimensional transverse NOE spectroscopy. *J. Magn. Reson.* 1985; **63**: 207–213.
21. Wüthrich K. *NMR of Proteins and Nucleic Acids*. John Wiley: New York, 1986.
22. Wishart DS, Bigam CG, Holm A, Hodges RS, Sykes BD. H-1, C-13 and N-15 random coil NMR chemical shifts of the common amino acids. 1. Investigations of nearest neighbor effects. *J. Biomol. NMR* 1995; **5**: 67–81.
23. Baxter NJ, Williamson, MP. Temperature dependence of ¹H chemical shifts in proteins. *J. Biomol. NMR* 1997; **9**: 359–369.
24. Weliky DP, Bennett AE, Zvi A, Anglister J, Steinbach PJ, Tycko R. Solid-state NMR evidence for an antibody-dependent conformation of the V3 loop of HIV-1 gp120. *Nat. Struct. Biol.* 1999; **6**: 141–145.
25. Petkova AT, Ishii Y, Balbach JJ, Antzutkin ON, Leapman RD, Delaglio F, Tycko R. A structural model for Alzheimer's beta-amyloid fibrils based on experimental constraints from solid state NMR. *Proc. Natl Acad. Sci. USA* 2002; **99**: 16 742–16 747.
26. Ruff MR, Polianova M, Yang Q, Leoung GS, Ruscetti FW, Pert CB. Update on D-Ala-Peptide T-Amide (DAPTA): A viral entry inhibitor which blocks CCR5 chemokine receptors. *Curr. HIV Res.* 2003; **1**: 51–67.